$$\Delta E_{12}^{\infty} = \Delta E_{12}^{\circ} + 0.09182\left(\frac{\exp(-\kappa R_2)}{1+\kappa R_1} + \frac{\exp(-\kappa R_1)}{1+\kappa R_2}\right) \times \left(\frac{Z_1Z_2 - Z'_1Z'_2}{R_1 + R_2}\right)$$

(20) (a) Marcus, R. A.; Sutin, N. *Inorg. Chem.* **1975**, *14*, 213. (b) Marcus, R. A. *J. Phys. Chem.* **1963**, *67*, 853.

(21) For nonadiabatic electron transfer reactions the Marcus relationship (neglecting *f*) is

$$\frac{k_{12}}{p_{12}} = \left(\frac{k_{11}}{p_{11}}\frac{k_{22}}{p_{22}}K_{12}\right)^{1/2}$$

This general expression reduces to eq 5 if the reactions in question are "uniformly nonadiabatic" ($p_{12}^2 = p_{11}p_{22}$) (Sutin, N. *Acc. Chem. Res.* **1968**, *1*, 225).

(22) In terms of the Hopfield formalism, use of the protein self-exchange rate constant fulfills the assumption of equivalent sites. Furthermore, because this stratagem removes dependence of the rate on the kinetic properties of the inorganic complex, it eliminates the uncertainty in the values of the parameters[10] that describe the small molecule site characteristics.

(23) Sailasuta, N.; Anson, F. C.; Gray, H. B. *J. Am. Chem. Soc.* **1979**, *101*, 455.

(24) The selection of 3.7 Å as the "closest contact" distance assumes that stellacyanin employs a self-exchange mechanism involving electron transfer through an imidazole ring of a histidine ligand. Alternatively, the protein may employ a mechanism involving a sulfur ligand (as is likely the case for the Fe–S proteins considered). In either case, the "closest contact" distance would be the same, since the van der Waals radius for S is also 1.85 Å. Thus, the calibration based on a 3.7-Å "closest contact" distance should be adequate for all reactions in which redox site contact occurs between aromatic carbon atoms (imidazole edges, heme edges) or sulfur atoms. The relevant structural data on cytochrome *c*[15,17] and HiPIP[15,18] have been discussed previously. The available structural information on the blue copper centers in plastocyanin, azurin, and stellacyanin has been reviewed recently (Gray, H. B. *Adv. Inorg. Biochem.* **1979**, *2*, 1).

(25) Put another way, we assume that the rate constants depend on the "nonadiabatic distance" of electron transfer as follows:

$$k_{12} = k_{12}^{\circ}\,[\exp(-2aR_1)]\,[\exp(-2aR_2)]$$

where k_{12}° is the rate constant that would be observed if the reaction were adiabatic (R_1, $R_2 = 0$) and R_1 and R_2 are the "nonadiabatic distances" for reactants 1 and 2, respectively. In our analysis $2R_p = 3.7$ Å for $R_1 = 0$.

(26) Even though the apoprotein does not impose any protein–reagent interactions on the kinetics of the blue copper center in stellacyanin, it does limit the surface area of the copper center that is available for reaction. This statistical factor is a major determinant of the absolute magnitude of k_{11}^{∞}. Sutin has treated this effect in detail for cytochrome *c* by showing that the self-exchange rate constant for the protein ($\sim 10^3$ M^{-1} s^{-1}) compared to that for $Fe(phen)_3^{3+}$ ($\sim 10^7$ M^{-1} s^{-1}) is consistent with crystallographic data showing that about 3% of the porphyrin surface is available for electron transfer (N. Sutin, "Bioinorganic Chemistry-II", *Adv. Chem. Ser.* **1977**, *No. 162*, 156). A similar comparison of the self-exchange rate constant for stellacyanin ($\sim 10^5$ M^{-1} s^{-1}) with that for $Fe(phen)_3^{3+}$ ($\sim 10^7$ M^{-1} s^{-1}) would suggest that roughly 10% of the copper center "surface" is available for electron transfer in this protein. The use of a single value of *C* for all calculations based on eq 3 implies that the same statistical factor holds for all the proteins considered. This assumption should be nearly valid for cases involving hydrophilic (nonpenetrating) reagents. However, the potential ability for penetrating (hydrophobic) reagents to sample a larger relative "surface area" of a "buried" site may contribute to a larger uncertainty in the *R* values calculated for proteins reacting with these reagents. The penetration of such reagents may also contribute to changes in the Franck–Condon factors (which are implicitly included in the constant *C*) and this would also introduce error in the calculated *R* values.

(27) Sutin, N. "Inorganic Biochemistry", Eichhorn, G. I., Ed.; Elsevier: Amsterdam, 1973; p 611.

(28) The possible mechanisms that give rise to saturation behavior have been enumerated (Yoneda, G. S.; Holwerda, R. A. *Bioinorg. Chem.* **1978**, *8*, 139): (a) precursor complex formation, (b) rate-limiting formation of an activated form of the protein, and (c) dead-end complex formation.

(29) This value of the formation constant was calculated by extrapolation (linear in $\mu^{1/2}$) of the ionic strength dependent values given by Miller and Cusanovich (Miller, W. G.; Cusanovich, M. A. *Biophys. Struct. Mech.* **1975**, *1*, 97).

(30) Stellwagen, E.; Cass, R. D. *J. Biol. Chem.* **1975**, *250*, 2095.

(31) Potasek, M. J.; Hopfield, J. J. *Proc. Natl. Acad. Sci. U.S.A.* **1977**, *74*, 3817.

Cobalt Metallacycles. 8.[1] Preparative and Kinetic Studies on the Reactivity of Cobaltacyclopentadienes with Phosphites

Katsutoshi Yasufuku,* Akihiko Hamada, Katsuyuki Aoki, and Hiroshi Yamazaki

Contribution from the Institute of Physical and Chemical Research, Wako-shi, Saitama 351, Japan. *Received September 21, 1979*

Abstract: (η^5-Cyclopentadienyl)(triphenylphosphine)cobaltacyclopentadiene complexes, ($\overline{CoCR^1{=}CR^2CR^3{=}CR^4}$)($\eta^5$-$C_5H_5$)($PPh_3$) (**1**), react with phosphites, $P(OR^5)_3$ (**2**), yielding in successive steps (η^5-cyclopentadienyl)(phosphite)cobaltacyclopentadiene complexes, ($\overline{CoCR^1{=}CR^2CR^3{=}CR^4}$)($\eta^5$-$C_5H_5$)[$P(OR^5)_3$] (**3**) and isomeric 1-alkoxyphosphole oxide complexes (**4**). The structure of one isomer of the 1-methoxyphosphole oxide complex, **4ca-2**, was determined by an X-ray crystallographic structural analysis. The complexes **4**, when oxidized by Ce^{4+} ions, give 1-alkoxyphosphole oxides. Kinetic studies on the formation of **3** and of the conversion of **3** to **4** have been carried out and a first-order reaction has been verified in the complex concentration for both steps. Activation parameters for the reaction of **1c** (R^1, R^2, R^3, R^4 = Ph) with **2a** ($OR^5 = OCH_3$) are determined as $\Delta H^{\ddagger} = 31$ kcal mol^{-1} and $\Delta S^{\ddagger} = 4$ eu for the substitution, and as $\Delta H^{\ddagger} = 22$ kcal mol^{-1} and $\Delta S^{\ddagger} = -4$ eu for the conversion step, respectively. The preparative and kinetic investigations show that (1) both steric and electronic factors of the substituents of the cobalt metallacycles govern the substitution step, and (2) the electronic factor chiefly governs the conversion step. The steric effect of the alkyl groups of **2** is very distinctive in the conversion step.

I. Introduction

Cobaltacyclopentadienes have been considered to be key intermediates in the cobalt-catalyzed reactions of acetylenes.[2-4] Studies on the reactions of the stable (η^5-cyclopentadienyl)(triphenylphosphine)cobaltacyclopentadiene complexes, ($\overline{CoCR^1{=}CR^2CR^3{=}CR^4}$)($\eta^5$-$C_5H_5$)($PPh_3$) (**1**), with various unsaturated organic reagents L such as acetylenes,[5,6] olefins,[7] or compounds having a hetero multiple bond[8-10] have contributed to the understanding of the cobalt catalysis. In the catalytic process, it is believed that the L should first ligate on the cobalt by displacing the PPh_3 ligand to give an intermediate **3** (Scheme I). Then the intermediate **3** may be converted to a final product via insertion of L into the cobalt metallacycle. However, when L is an acetylene, another path involving a coordinated Diels–Alder type addition reaction cannot be excluded.

The production of **3** as an intermediate has been postulated for most of these systems and recently the first step of the reaction, substitution of PPh_3 with L, has been proven to be dissociation controlled in the reaction of **1** (R^1, R^2, R^3, R^4 = Me) with 2-butyne.[11] However, little is known about the reactivities of the cobalt metallacycles toward the reagent L or about the factors governing the reactions, particularily with

0002-7863/80/1502-4363$01.00/0

Table I. (Phosphite)cobaltacyclopentadiene Complexes (3), ($\overline{CoCR^1{=}CR^2CR^3{=}CR^4}$)($\eta^5$-$C_5H_5$)[P($OR^5$)$_3$]

compd	mp, °C	anal. found (calcd), % C	anal. found (calcd), % H	^{1}H NMR, δ, ppm (J_{PH}, Hz)^a η^5-C_5H_5	POCH$_n$	other aliphatic protons
3ba	152–154	68.76 (68.63)	6.07 (5.95)	4.45 (s)^c	3.63 (d, 11.2)	1.59 (CMe, d, 1.6)
3ca	189–190	71.55 (71.52)	5.91 (5.67)	4.67 (s)	3.60 (d, 10.6)	
3cb	182–184	72.44 (72.44)	6.27 (6.24)	4.66 (s)	3.92 (d of q, 7.0, J_{HH} = 7.0)^d	1.25 (Me, t, J_{HH} = 7.0)
3cc	169–172	73.43 (73.24)	6.72 (6.77)	4.68 (s)	4.56 (m, bd)	1.20 (Me, d, J_{HH} = 6.0)
3cd	202–204	74.21 (73.77)	5.72 (5.59)^b	4.56 (s)	4.25 (d, 5.0)	0.81 (Me, s)
3ce	162–165	72.13 (72.07)	5.64 (5.56)	4.58 (s)	3.66 (OMe, d, 10.8), 3.8–4.8 (OCH$_2$, m)	1.5–2.5 (CCH$_2$C, m, bd)
3cg	oil	75.89 (75.69)	5.79 (5.58)	4.89 (s)	3.47 (d, 9.8)	
3ch	167–170	79.17 (79.07)	5.24 (5.20)	4.58 (s)^c		
3fa	131–132	61.99 (61.84)	5.78 (5.76)	4.46 (s)	3.59 (d, 10.8)	1.84 (CMe, d, 1.4), 3.51 (CO$_2$Me, s)
3ga	199–201	65.66 (65.53)	5.51 (5.50)	4.59 (s)^c	3.62 (d, 11.0)	3.11 (CO$_2$Me, s)
3ha	185–187	59.70 (59.17)	5.44 (5.31)	4.96 (s)	3.64 (d, 10.8)	3.38 (CO$_2$Me, s)
3hd	237–238	61.01 (60.82)	5.14 (5.10)	4.49 (s)^c	4.27 (d, 5.4)	0.81 (CMe, s), 3.34 (CO$_2$Me, s)
3hh	214–216	64.99 (64.50)	5.38 (5.25)	4.38 (s)	3.47 (d, 10.0)	3.02 (CO$_2$Me, s)
3ia	139–140	59.40 (59.17)	5.38 (5.31)	4.79 (s)	3.70 (d, 10.8)	3.20, 3.42 (CO$_2$Me, s, s)

^{a} Shifts in CDCl$_3$ relative to internal Me$_4$Si. Phenyl signals are omitted. ^{b} Solvated with $\frac{1}{2}C_6H_6$. ^{c} Measured in CD$_2$Cl$_2$. ^{d} s = singlet, d = doublet, t = triplet, q = quartet, m = multiplet, bd = broad.

Scheme I

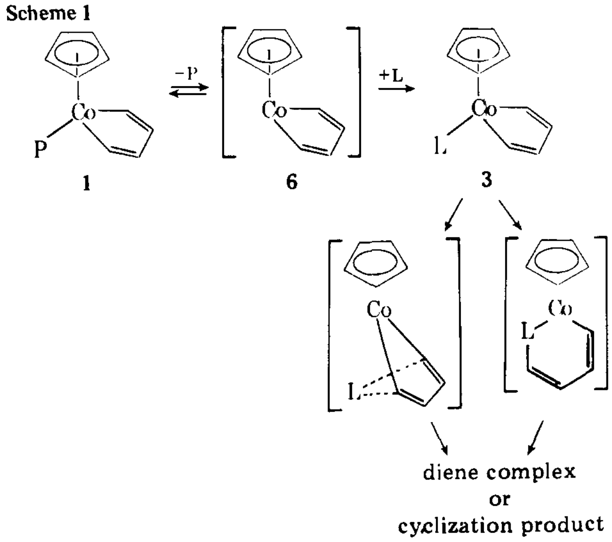

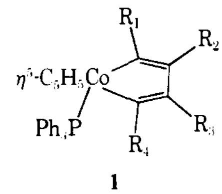

1

	R^1	R^2	R^3	R^4
1a	Ph	Me	Me	Ph
b	Ph	Me	Ph	Ph
c	Ph	Ph	Ph	Ph
d	Me	Me	Me	Me
e	Me	Me	Ph	Ph
f	Ph	Me	CO$_2$Me	Ph
g	Ph	Ph	CO$_2$Me	Ph
h	Ph	CO$_2$Me	CO$_2$Me	Ph
i	Ph	CO$_2$Me	Ph	CO$_2$Me

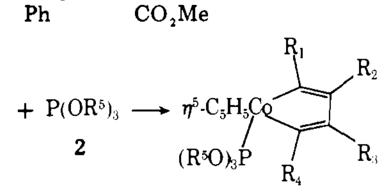

(1)

2a P(OMe)$_3$
b P(OEt)$_3$
c P(OPr^i)$_3$
d $\overline{P(OCH_2)_3CCH_3}$
e $\overline{P(OCH_2CH_2O)}$(OMe)
f $\overline{P(OCH_2CH_2O)}$(OMe)
g P(OPh)$_3$
h PPh(OMe)$_2$
i PPh(OPh)$_2$

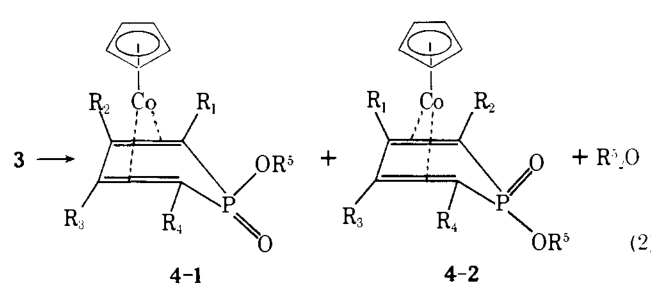

(2)

respect to the second conversion step. This might be attributed mainly to the lack of isolation of spectral detection of the intermediates **3** so far.

We have found that the reaction of **1** with phosphites **2** gives (η^5-cyclopentadienyl)(1-alkoxyphosphole oxide)cobalt complexes **4** via phosphite-substituted cobaltacyclopentadienes **3**. The isolation of **3** has enabled us to carry out the kinetic studies of the substitution and the conversion steps independently by means of ^{1}H NMR spectroscopy. The reaction mechanism and factors governing each individual step are discussed from the preparative and the kinetic point of view.

II. Results

1. Preparative Investigations. (a) Formation of (η^5-Cyclopentadienyl)(phosphite)cobaltacyclopentadienes 3 and (η^5-Cyclopentadienyl)(1-alkoxyphosphole oxide) Cobalt Complexes 4. The reaction of (η^5-cyclopentadienyl)(triphenylphosphine)cobaltacyclopentadienes **1** with phosphites **2** gives **4** through formation of **3** according to eq 1 and 2.

The reaction is classified into three categories depending on the substituents in **1** and on the nature of **2**: (1) systems where **3** is not observed in the **1** + **2** → **4** reaction (**1a** or **1d** with **2a**, **1c** with **2e**, and **1c** with **2g**); (2) a system where **1** + **2** gives **3**; however, **3** cannot give **4** (the reaction system with **2c**); and (3) systems where **1** + **2** give in stepwise fashion **3** and **4** which were isolated or observed (most reaction systems tried fell into this category). The systems give **3** under mild reaction conditions followed by a conversion of the isolated **3** to **4** under more vigorous reaction conditions in the presence of excess **2**. The complexes **3** and **4** thus obtained are shown in Tables I[12] and II, respectively.

All phosphole oxide complexes **4** from **1a–f** were found, by

Table II. Physical Properties and Analytical Data of 1-Alkoxyphosphole Oxide Complexes (**4**), $Co(\eta^5\text{-}C_5H_5)[R^5O\overline{P(O)CR^1{=}CR^2CR^3{=}C}R^4]$

compd	mp, °C	anal. found (calcd), % C	anal. found (calcd), % H	IR,[a] $\nu_{P=O}$, cm^{-1}	^1H NMR, δ, ppm (J_{PH}, Hz)[b] $\eta^5C_5H_5$ $POCH_n$	other aliphatic protons
4aa-1	242–243	66.28 (66.37)	5.62 (5.57)	1180	4.66 (s) 3.74 (d, 10.8)	2.26 (CMe, s, bd)
4aa-2	231–232	66.57 (66.37)	5.62 (5.57)	1213	4.72 (s) 3.20 (d, 10.8)	2.38 (CMe, s, bd)
4ba-2[c]	118–119	71.56 (71.78)	5.82 (5.45)[e]	1213	4.80 (s) 3.41 (d, 10.8)	2.24 (CMe, s, bd)
4ca-1	297–298	73.52 (73.12)	5.23 (5.05)	1198	4.87 (s) 3.92 (d, 11.4)	
4ca-2	226–228	73.55 (73.12)	5.29 (5.05)	1219	4.92 (s) 3.49 (d, 10.6)	
4cb-1	275–277	73.36 (73.42)	5.48 (5.28)	1205	4.93 (s) 4.30 (d of q,[g] 7.0, J_{HH} = 7.0)	1.40 (Me, t, J_{HH} = 7.0)
4cb-2	226–230	73.18 (73.42)	5.57 (5.28)	1220	4.90 (s) 3.80 (d of q, 9.0, J_{HH} = 7.0)	1.06 (Me, t, J_{HH} = 7.0)
4cd-1	246–247	74.49 (74.78)	5.80 (5.70)[f]	1205	4.93 (s) 4.12 (d, 3.6)	4.51 (CCH_2O, AB,[h]) 1.35 (CMe, s)
4cd-2	200–202	72.49 (72.61)	5.57 (5.46)	1223	4.90 (s) 3.79 (d, 4.8)	4.21 (CCH_2O, AB,[i]) 1.13 (CMe, s)
4cg-1	320–321	75.42 (75.48)	4.94 (4.87)	1220	4.92 (s)	
4cg-2	241–242	75.59 (75.48)	4.92 (4.87)	1230	4.87 (s)	
4ch-1	299–302	77.50 (77.49)	5.17 (5.00)	1202	5.00 (s)	
4ch-2	335–339	77.39 (77.49)	5.20 (5.00)	1170	4.71 (s)	
4da-1[c]					4.50 (s) 3.87 (d, 10.0)	1.34 (α-CMe, d, 13.2), 1.99 (β-CMe, s)
4da-2	174–176	54.60 (54.21)	6.53 (6.51)	1205	4.65 (s) 3.24 (d, 9.6)	1.36 (α-CMe, d, 13.2), 2.06 (β-CMe, d, 0.5)
4ea-1	*d*	66.04 (66.37)	5.70 (5.57)	1200	4.73 (s) 3.94 (d, 11.2)	1.58 (α-CMe, d, 13.2), 2.00 (β-CMe, s, bd)
4ea-2	oil	*j*		1213	4.83 (s) 3.40 (d, 11.2)	1.57 (α-CMe, d, 13.2), 2.04 (β-CMe, d, 0.5)
4fa-2[c]	*d*	63.20 (62.77)	5.53 (5.06)	1213	4.94 (s) 3.29 (d, 11.2)	2.42 (CMe, s, bd), 3.81 (CO_2Me, s)
4ha	243–245	59.43 (59.78)	4.73 (4.63)	1228	4.94 (s) 3.32 (d, 11.4)	3.81 (CO_2Me, s)
4hg	162–164	64.02 (63.71)	4.54 (4.48)	1220	4.92 (s)	3.72 (CO_2Me, s)
4hh	111–113	65.68 (65.50)	4.70 (4.61)	1210	4.90 (s)	
4ia	*d*	59.48 (59.78)	4.85 (4.63)	1220	5.05 (s) 3.53 (d, 11.4)	3.54, 3.67 (CO_2Me, s, s)

[a] In KBr. [b] Shifts in $CDCl_3$. Phenyl signals are omitted. [c] The minor isomer detectable in ^1H NMR spectra was not isolated. [d] Noncrystalline solid. [e] Solvated with $\frac{1}{2}C_6H_6$. [f] Solvated with C_6H_6. [g] s = singlet, d = doublet, t = triplet, q = quartet, bd = broad. [h] $|\nu_{AB}|$ = 15.3 Hz, J_{AB} = 4.8 Hz. [i] $|\nu_{AB}|$ = 3.6 Hz, J_{AB} = 5.2 Hz. [j] Analysis was not made.

NMR spectroscopy, to consist of two isomers, some of which were isolated by chromatographic separation using a C_6H_6-ethyl acetate mixture of variable portions as an eluant. The more readily eluted isomers, **4–1**, which were produced in minor portions, show higher melting points and lower IR spectral band wavenumbers corresponding to P=O stretching than those of the less elutable major isomers, namely, **4-2**; the isomers **4ch-1** and **4ch-2** were exceptions to this characterization.

4ca-1, **4cb-1**, and **4cg-1** isomerized to the other isomers when heated neat to 280–300 °C, whereas no isomerization corresponding to **4-2** → **4-1** occurred, showing **4-2** to be thermodynamically stable. No isomerization of **4-1** to **4-2** in the preparative conditions suggests that the formation of **4** is kinetically controlled.

(b) **Structure of 4ca-2.** Single-crystal X-ray analysis of the structure of **4ca-2** determined it to be the *exo*-1-methoxy isomer. The molecular geometry and the numbering scheme used for nonhydrogen atoms are shown in Figure 1. The structure shows η^4 coordination of the phosphole ring to the Co atom with distances between the Co and the C(2)-C(3)-C(4)-C(5) plane being 1.594 Å, the P atom being 0.632 Å away from the plane, and the 1-methoxy group occupying the exo position relative to the Co atom with the distances P-O(1), 1.607 Å, O(1)-C(1), 1.441 Å, and P-O(2), 1.484 Å. The selected bond distances and angles are shown in Table VI. These are comparable to those of $(\eta^5\text{-}C_5H_5)Co[\eta^4\text{-}(CF_3)_4C_4P(O)OH]$[13] except for the geometry around P(O)OH.

Consequently the structure of **4ca-1** should be the *endo*-1-methoxy isomer. Thus we tentatively classify the structure of the isomer series **4-2**, having higher $\nu_{P=O}$ values, as exo and the other series **4-1**, having lower $\nu_{P=O}$, as endo isomers. In the case of **4ch**, the more readily eluted isomer has a higher $\nu_{P=O}$ value and should be classified as the exo isomer, and the less readily eluted isomer **4ch-2** as an endo isomer. The reverse of the elution order of **4ch** compared to other 1-alkoxyphosphole

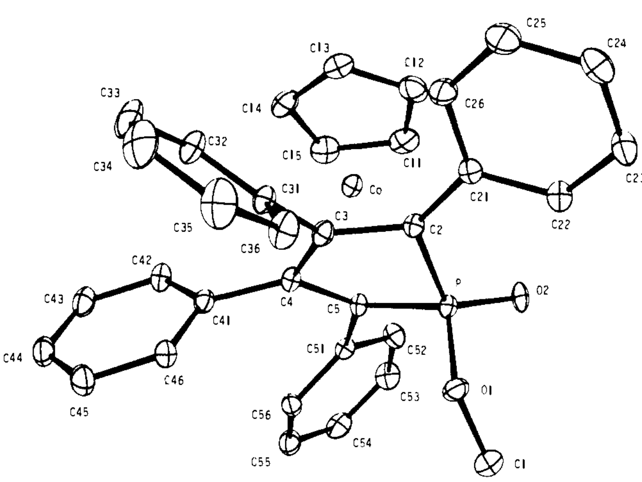

Figure 1. Molecular geometry of **4ca-2**.

oxide complexes may be attributed to the difference of the bond polarities between the P-Ph and P-OR.

(c) **Formation of Phosphole.** The complexes **4** were cleaved by oxidation with Ce^{4+} ion or iodine, when the substituents of **4** were phenyls and/or methyls, yielding phosphole oxides[14] in good yields, whose properties are shown in Table III. The phosphole oxide complexes having methoxycarbonyl substituents, however, could not be cleaved under the conditions.

2. Kinetic Investigation. The isolation of the intermediate complexes **3** has enabled us to investigate the factors influencing the substitution step (reaction 1) and the conversion step (reaction 2) individually, by means of ^1H NMR spectrometry in which the signal heights of the $\eta^5\text{-}C_5H_5$ protons of the starting and product complexes are measured.

(a) **Substitution Step.** The rate of the substitution reaction of **1c** was independent of the nature of the phosphites (except

Table III. 1-Alkoxyphosphole Oxides, $R^5O\overline{P(O)CR^1{=}CR^2CR^3{=}C}R^4$

R^1	R^2	R^3	R^4	OR^5	color	mp, °C	anal. found (calcd), % C	H	^1H NMR, δ, ppm (J_{PH}, Hz)[a]
Ph	Ph	Ph	Ph	OMe	yellow	208-210	80.00 (80.16)	5.44 (5.34)	3.79 (OMe, d, J_{PH} = 11.0)
Ph	Ph	Ph	Ph	OEt	yellow	196-197	80.11 (80.36)	5.67 (5.62)	4.10 (OMe, d of q, J_{PH} = 7.2, J_{HH} = 7.0) 1.22 (Me, t, J_{HH} = 7.0)
Ph	Ph	Ph	Ph	OPh	yellow	188-189	82.30 (82.24)	5.07 (5.07)	
Ph	Ph	Ph	Ph	Ph	yellow	270-271[b]	84.84 (84.98)	5.32 (5.24)	
Ph	Ph	Ph	Ph	CH_3 OCH_2C—CH_2 CH_2—O	yellow	200-203	78.48 (78.51)	5.92 (5.79)	4.03 (POMe, d, J_{PH} = 4.8) 4.31 (CCH_2O, AB)[c] 1.18 (CMe, s)
Ph	Me	Me	Ph	OMe	colorless	153-154	73.29 (73.52)	6.14 (6.16)	3.50 (OMe, d, J_{PH} = 10.8) 2.13 (CMe, d, J_{PH} = 2.5)
Me	Me	Me	Me	OMe	colorless	oil	58.48 (58.06)	8.34 (8.10)	3.64 (OMe, d, J_{PH} = 11.5) 1.85 (α-CMe, d, bd, J_{PH} ~12) 1.87 (β-CMe, s, bd)

[a] In $CDCl_3$; phenyl protons are omitted. [b] Lit. 292-293,[15] 284-285 °C.[16] [c] $|\nu_{AB}|$ = 6.8 Hz, J_{AB} = 5.4 Hz.

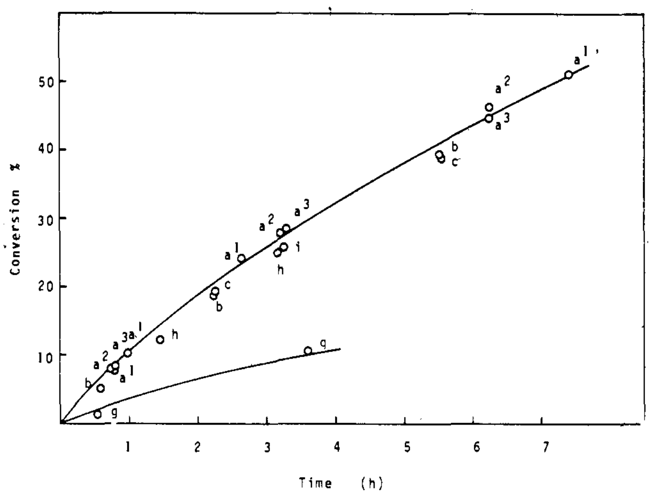

Figure 2. The reaction rate of **1c** (1.2×10^{-1} M) with various phosphites: a, **2a** (a[1] 1.9×10^{-1} M, a[2] 12.2×10^{-1} M, a[3] 5.5×10^{-1} M); b, **2b**; c, **2c**; g, **2g**; h, **2h**; i, **2i** (2×10^{-1} M for b–i), in CD_2Cl_2 at 62 °C.

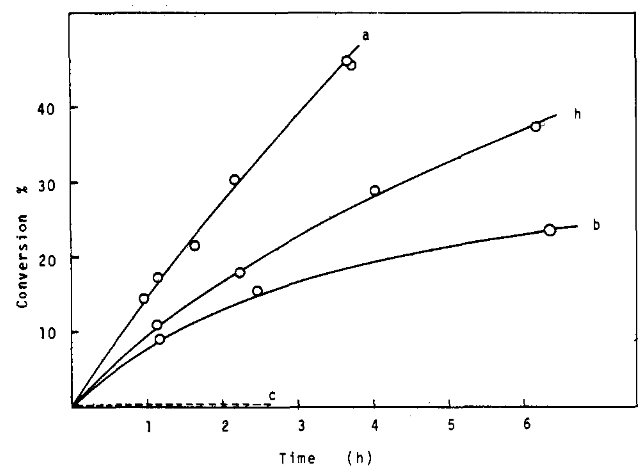

Figure 3. The effect of the coordinated phosphite on the rate of **4** formation from **3** (1.4×10^{-1} M) in the presence of corresponding **2** (1.8×10^{-1} M) at 100 °C in CD_2Cl_2: a, **3ca**; b, **3cb**; c, **3cc**; h, **3ch**.

2g) and independent of [**2a**], within a range of 1.5–10 molar equiv [**1c**] as shown in Figure 2.[17] This suggests the substitution reaction to be first order in [**1c**] and zero order in concentration of phosphite. The first-order rate constants for the reactions of seven cobaltacyclopentadiene complexes with **2a** are listed in Table IV. The rate constants for the system of **1a**, **1d**, and **1e** were estimated with the assumption that the formation of **4aa**, **4da**, and **4ea** is controlled by dissociation; however, only a qualitative estimation was possible because of the occurrence of appreciable signal broadening in the spectra. In the case of **1b**, the appearance of the signal due to η^5-C_5H_5 of **3ba** followed by growth of the signals due to the formation of **4ba** was observed. The rate of formation was estimated by the change in the summed heights of these signals. In the case of **1h** having two methoxycarbonyls, the rate was not only low but also deviated appreciably from the simple first-order expression, so the value for **1h** was obtained by applying an initial-rate method. These qualitative values are shown in parentheses in Table IV for comparison.

(b) Conversion Step. As will be described in the Experimental Section, this step is accompanied by the formation of η^4-cyclobutadiene complexes **5** as a side reaction. However, this side reaction can be suppressed by adding phosphite to the system, permitting kinetic measurements of the conversion step. The conversion of **3ca** to **4ca** was found to obey first-order kinetics within a wide range of [**2a**]. The system of **3ba** also shows first-order kinetics. The first-order rate constants and activation parameters for these systems are shown in Table V.

The percent conversion in the reaction of tetraphenylcobaltacyclopentadiene complexes having several phosphites is shown in Figure 3 as a function of reaction time. The rate of this conversion is very dependent on the nature of the phosphite coordinated. When the ligand was **2b** or **2h**, the reaction was slower than that for **2a** and also was found to deviate appreciably from first-order kinetics. In the system with **2c**, the formation of **4cc** was undetectable because a considerable signal broadening occurred from an early stage in the reaction.

III. Discussion

1. Substitution Reaction. The reactivities of the cobaltacyclopentadienes are compared in Table IV by means of the k values for the reaction with **2a**. Further, the rates of the reaction with PEt_3 were also measured and the results are included in Table IV. Since only substitution occurs with PEt_3, more precise k values than those obtained with **2a** could be determined for the cobaltacyclopentadienes having the electron-releasing methyl group. The system of **1d** and PEt_3 showed considerable signal broadening which prevented the rate estimation in CD_2Cl_2. There was no such impediment for the rate determination in C_6D_6.

Table IV. Dissociation Rate Constants and Activation Parameters for the Reaction of **1** with L in CD_2Cl_2

	$k_{°C} \times 10^{-5}$, s^{-1}		$\Delta H^{\ddagger}$,	$\Delta S^{\ddagger}$,
	L = PEt_3	L = $P(OMe)_3$	kcal mol^{-1}	eu
1a	$k_{55.1}{}^{a} = 17.3 \pm 0.7$		30.4 ± 0.2	4.1
	$k_{50.1} = 8.2 \pm 0.1$	($k_{60} > 25$)		
	$k_{45.0} = 3.8 \pm 0.1$			
1b	$k_{61.0}{}^{b} = 12.1 \pm 0.1$		30.6 ± 0.2	3.7
	$k_{55.0} = 5.2 \pm 0.1$	($k_{60} \sim 14$)		
	$k_{50.1} = 2.5 \pm 0.1$			
1c	$k_{70.0}{}^{c} = 8.5 \pm 0.2$	$k_{70.0}{}^{e} = 9.3 \pm 0.2$	31.6 ± 0.2	3.7
	$k_{65.1} = 4.4 \pm 0.1$	$k_{65.1} = 5.0 \pm 0.1$		
	$k_{61.0} = 2.4 \pm 0.1$	$k_{59.7} = 2.1 \pm 0.1$		
1d	$k_{76.0}{}^{d} = 8.2 \pm 0.2$		31.7 ± 0.3	3.4
	$k_{70.0} = 3.6 \pm 0.1$	($k_{80} \sim 11$)		
	$k_{61.0} = 1.0 \pm 0.1$			
1e		($k_{69} = 3.0$)		
1f		$k_{87.5}{}^{f} = 22.3 \pm 1.2$	33.9 ± 0.4	4.5
		$k_{79.5} = 7.5 \pm 0.1$		
		$k_{69.5} = 1.8 \pm 0.1$		
1h		($k_{100} \sim 2$)		

Experimental conditions: [a] [**1a**] 1.23×10^{-1} M; [b] [**1b**] 1.11×10^{-1} M; [c] [**1c**] 1.04×10^{-1} M; [d] [**1d**] 1.28×10^{-1} M, in C_6D_6, in the presence of [PEt_3], 4.2×10^{-1} M; [e] [**1c**] 1.04×10^{-1} M; [f] [**1f**] 1.37×10^{-1} M in the presence of [**2a**], 4.2×10^{-1} M.

Table V. Rate Constants and Activation Parameters for Conversion Reactions, **3** → **4** in CD_2Cl_2

	$k_{°C}$ $\times 10^{-5}$, s^{-1}	$\Delta H^{\ddagger}$, kcal mol^{-1}	$\Delta S^{\ddagger}$, eu
3ba[a]	$k_{70.1} = 9.5 \pm 0.1$	19.7 ± 0.2	-3.9
	$k_{65.2} = 6.2 \pm 0.1$		
	$k_{59.7} = 3.7 \pm 0.1$		
3ca[b]	$k_{116.9} = 15.7 \pm 0.2$	22.3 ± 0.2	-3.8
	$k_{110.0} = 9.2 \pm 0.2$		
	$k_{99.9} = 4.0 \pm 0.1$		
3fa[c,e]	$k_{129.8} = 20.4$	~24	
	$k_{120.0} = 9.0$		
	$k_{110.0} = 4.2$		
3ga[d,e]	$k_{139.6} = 8.8$	~26	
	$k_{129.8} = 3.6$		
	$k_{120.0} = 1.7$		

Experimental conditions: [a] [**3ba**] 1.44×10^{-1} M and [**2a**] 4.2×10^{-1} M; [b] [**3ca**] 1.66×10^{-1} M and [**2a**] 3.2×10^{-1} M; [c] [**3fa**] 1.18×10^{-1} M and [**2a**] 4.2×10^{-1} M; [d] [**3ga**] 1.36×10^{-1} M and [**2a**] 3.0×10^{-1} M. [e] The constants were estimated by initial rate method.

There is a slight difference in the k values for the system of **1c** with PEt_3 and of **1c** with **2a**; however, both series of k values result in the same value of $\Delta H^{\ddagger} \sim 31$ kcal mol^{-1} and $\Delta S^{\ddagger} \sim 4$ eu, indicating that we can consider in detail the factors influencing the reactivity of the cobaltacyclopentadienes in terms of the k values from both systems.

(a) Reactivity of Incoming Ligands in the Substitution. The substitution of PPh_3 in **1d** with PEt_3 has been shown by Bergman et al.[11] to be first order in [**1d**] and independent of [PEt_3]. The present work verifies that first-order kinetics is fulfilled in the reaction of **1c** with a wide range of phosphites and phosphonites as well as PEt_3 (except **2g**), and also in the reaction of a series of the cobaltacyclopentadienes with **2a** and PEt_3 (except **1h** and **1i**). The first-order kinetics is attained by providing the incoming ligand **2** at a high rate to scavenge **6** eliminating the back-reaction to **1.**

$$\mathbf{1} \underset{+PPh_3\ k_{-1}}{\overset{-PPh_3\ k_1}{\rightleftharpoons}} \mathbf{6} \xrightarrow{+\ 2\ k_2} \mathbf{3}$$

Under these conditions, the rate expression, $d[3]/dt = k_1k_2[1][2]/(k_{-1}[PPh_3] + k_2[2])$, becomes the simple first-order expression, $d[3]/dt = k_1[1]$, since $k_2 \gg k_{-1}$ and $[2] > [PPh_3]$. The high reactivity of the incoming ligands to **6**, compared to that of PPh_3, may be mainly due to the difference in size of the ligands,[18] in comparison with those of PPh_3, rather than the difference in the donor–acceptor properties. However, in the case of **2g**, which was also smaller than PPh_3 in size, the reactivity was not high compared to that of PPh_3. The weaker basicity and the bulkiness of **2g** can be taken together to account for the lower reactivity and the deviation from the simple first-order kinetics, through competition with PPh_3 toward **6.** Both **2c** and PEt_3 follow first-order kinetics despite **2c** having a cone angle similar to that of **2g,** and PEt_3 even larger than **2g.** The stronger donor ability of **2c** and PEt_3, relative to **2g,** may explain these observations.

(b) Reactivity of the Cobaltacyclopentadienes. The reactivity order of a series of the cobaltacyclopentadienes in the PPh_3 substitution with **2a** is thus found as shown in Chart I.

α,α'-Diphenyl-β,β'-dimethylcobaltacyclopentadiene complex A is the most reactive and the activity decreases along the illustrated order to those having two methoxycarbonyl groups. It is obvious that the substituent of the cobalt metallacycle which enhances the electron density on the Co atom may make the P-Co bond weaker and vice versa. This electronic consideration explains the reactivity order among A, B,

Chart I

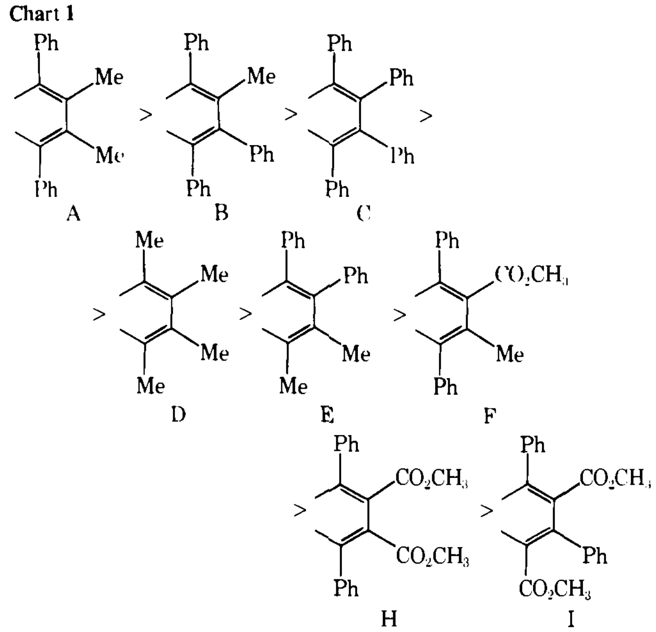

Scheme II

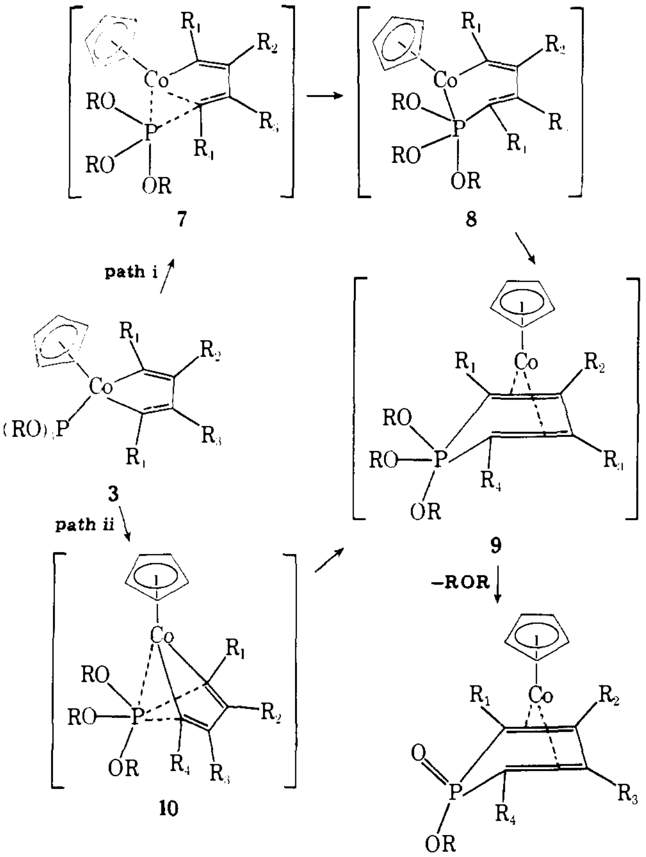

C, F, and H. However, the observed order also reveals another factor. By the electronic considerations, D is expected to be the most reactive. However, this is not the case. Thus the observed reactivity suggests a steric enhancement of the dissociation rate due to the presence of phenyl groups in α,α' positions. A single α-phenyl does not show such an effect as can be seen in E and I.

It is noteworthy that the reactivity order, D > A > B > C, has been found in the photochemical experiments. Under such conditions, the electronic factor of the substituents may predominate.

2. Conversion Reaction. The kinetic results and the absence of a solvent effect on the reaction rate, **3ca** → **4ca,** using CD_2Cl_2, C_6H_5Cl, and a $(CD_3)_2CO$-CD_2Cl_2 (2/1) mixture as a solvent, lead us to propose Scheme II.

Although formation of the 1-trialkoxyphosphole complex **9** was not detected, the formation of **9** and successive facile elimination of ether giving **4** are proposed, based on isolation of (η^5-cyclopentadienyl)(1-trifluorophosphole)cobalt complex in the reaction of $(\eta^5\text{-}C_5H_5)Co(PF_3)_2$ with $CF_3C{\equiv}CCF_3$.[19] The elimination of ether was suggested in NMR spectra of the reaction systems of **2a,** showing the appearance of a signal assignable to CH_3OCH_3 at δ 3.22 in CD_2Cl_2, and was confirmed by the reaction of **3cd** heated neat, giving **4cd,** in which the eliminated ether moiety is attached as the oxetane ring.

9 may be formed by either path i or ii. Path i involves an insertion of the coordinated phosphite into the Co-carbon bond giving a ring-enlarged **8** through **7** by an intramolecular oxidative addition of the Co-C bond to the phosphorus atom and a conversion of **8** to **9** by a reductive coupling of the phosphorus and another α carbon. Path ii involves a 1,4 cycloaddition of the phosphite to the α,α' carbons in the coordination sphere, **10.** The negative value for $\Delta S^{\ddagger}$ (−4 eu) for this reaction indicates the concerted nonionic intramolecular transformation to **7** or **10** without any bond splitting to be the rate-determining step.

Chart II

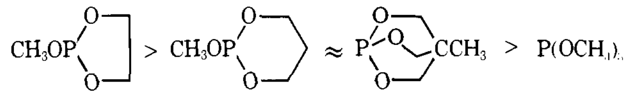

2e > **2f** ≈ **2d** > $P(OCH_3)_3$ **2a**

> $PPh(OCH_3)_2$ **2h** > $P(OC_2H_5)_3$ **2b** >> $P(OC_3H_7\text{-}i)_3$ **2c**

(a) Reactivity of Coordinated Phosphites. A characteristic of the conversion step is that the rate is very dependent on the nature of **2,** as shown in Figure 3. This contrasts with the substitution step, in which the rate is insensitive with respect to the nature of **2** used. The reactivity order of the phosphites is shown in Chart II. The order of the first two cyclic phosphites is suggested by the following arguments. Although both systems yielded mixtures of **4ca** and the 1-ω-hydroxyalkoxyphosphole oxide complexes instead of the expected 1-ω-methoxyphosphole oxide complexes, and although the mechanism for the formation of the ω-hydroxyalkoxy complexes is not clear, it may not be unreasonable to consider that the ω-hydroxyalkoxyphosphole oxide complexes as well as **4ca** are formed from the intermediate **9** after the rate-determining step. By this assumption, the faster disappearance of the η^5-C_5H_5 signal of **3cf** than that of **3ca** is considered to correspond to the higher reactivity of **3cf** compared to **3ca.** The reactivity of **2e** is considered highest because the corresponding **3ce** could not be isolated or detected. The relative reactivity of **2g** and **2i** could not be estimated even qualitatively by the NMR method, although it should be noted that they can be higher than that of **2c** since both **2g** and **2i** could yield the corresponding phosphole oxide complexes.

The reactivity order thus evaluated is opposite to those which have been found in the reactions ofphosphites involving the ionic intermediate of a four-valent phosphorus as seen in well-known Arbusov-type reactions.[20a] The characteristic order of the reactivity might be comparable to that found in the reaction of cyclic phosphines[21] or cyclic phosphites[22] with dialkyl peroxides, in which a transition state of the concertedly pentacoordinated phosphorus has been proposed.

It is known that trivalent phosphorus compounds with electronegative substituents undergo a facile addition to dienes to give pentavalent phospholene derivatives, and that phosphites can react with dienes only when the phosphite is cyclic.[20b] The reactivity of the coordinated phosphites in the conversion step can be attributed to the decreased electron density of the phosphorus by coordination to the Co atom of the formal charge of 3. The enhanced positive character of the coordinated **2** may facilitate the change in the valence of the P atom from a tetracoordinate P(III) to a pentacoordinate P(V).

The characteristic reactivity order, however, may be explained by the steric effect on the transformation from the tetrahedral tetracoordinate phosphorus to the bipyramidal pentacoordinate one. The ring strain present in the tetracoordinate state of the cyclic phosphites may be released in the pentacoordinate state; on the other hand, a steric constraint arising from the transformation of **2** having bulky groups may retard the formation of **7** or **10** and result in no formation of **4cc** from **3cc.**

(b) Reactivity of Cobaltacyclopentadienes toward 2a. The following reactivity order of the cobaltacyclopentadienes is deduced from the kinetic and photochemical observations:

D > A > B > C > F > G > H >> I

G = 1,2,4-triphenyl-3-methoxycarbonyl

A characteristic of the conversion reaction is that $\Delta H^{\ddagger}$ is smaller than that for the substitution reaction. Despite this, the conversion reaction of **3ca** requires a higher temperature than the substitution of PPh_3 does. This is attributable to the difference in the sign of $\Delta S^{\ddagger}$ for the individual steps. Because of the smaller activation enthalpy and the negative activation entropy for the conversion reaction, the first-order conversion rates of A and of D exceed the corresponding dissociation rates at the experimental conditions, which would result in preventing the isolation of **3aa** and **3da.**

The reactivity order may be attributed to the electronic effect of the substituents on the interaction between the α carbon and the electron-deficient phosphorus, and on the strength of the Co-carbon bond. Substitution with an electron-withdrawing group results in lower electron density for the α carbon and a stronger Co-C bond; these two factors result in a greater $\Delta H^{\ddagger}$ value and a conversion reaction which is competitive relative to dissociation of the phosphite ligand and therefore leading to degradations. When the cobalt metallacycle has methoxycarbonyl groups, the lower reaction rates, the deviations from first-order kinetics, and the broadening in the NMR spectra may arise from such side reactions.

IV. Experimental Section

1. General Procedures and Physical Measurements. The reactions were carried out under an atmosphere of nitrogen or argon. Melting points were taken on a Laboratory Devices Mel-Temp apparatus and are uncorrected. Infrared spectra were recorded on a Shimazu IR-27G spectrometer and ^1H NMR spectra were recorded with a JEOL C-60HL or Varian HA-100B spectrometer, using tetramethylsilane as a reference.

2. Materials. Triphenylphosphinecobaltacyclopentadiene complexes **1a–h** were prepared according to published methods.[7,11] Phosphites **2a–c** and **2g** were redistilled as commercial reagents which were stored under an atmosphere of argon after distillation. The phosphites **2d–f** and **2h,i** were prepared according to published methods.[23,24]

3. Preparation of Triphenylphosphinecobaltacyclopentadiene Complexes. In benzene (50 mL), $Co(\eta^5\text{-}C_5H_5)(PPh_3)(PhC{\equiv}CCO_2CH_3)$[25] (1.0 g, 2.0 mmol) and $PhC{\equiv}CCH_3$ (0.3 g, 2.6 mmol) were allowed to react at room temperature for 3 days. The color of the solution changed from reddish-brown to light brown. The reaction mixture was concentrated and chromatographed on alumina (1.5 × 15 cm). A brown band, eluted with benzene, was concentrated to 5 mL. The addition of hexane gave dark orange crystals (0.08 g): mp 209–210 °C; NMR ($CDCl_3$) δ 4.84 (C_5H_5, s), 2.88 (CO_2CH_3, s), 1.22 (CCH_3, s, bd), and 6.4–7.4 (C_6H_5, complex), suggesting the crystals to be the α-CO_2CH_3 and β-CH_3 isomer of **1f**; IR (KBr) 1676 cm^{-1} ($\nu_{C=O}$). Anal. Calcd for $C_{42}H_{36}O_2OCo$: C, 76.13; H, 5.48. Found: C, 76.43; H, 5.54.

The second brown band, eluted with a benzene-CH_2Cl_2 (7/1) mixture, gave dark brown crystals of **1f** (0.25 g): mp 194–196 °C; NMR δ 4.66 (C_5H_5, s), 3.24 (CO_2CH_3, s), 1.53 (CCH_3, d, J_{PH} = 1.4 Hz), and 6.4–7.4 (C_6H_5, complex); IR (KBr) 1693 cm^{-1} ($\nu_{C=O}$). Anal. Found: C, 76.50; H, 5.90.

1e was prepared similarly from $Co(\eta^5\text{-}C_5H_5)(PPh_3)(PhC{\equiv}CPh)$ (1.0 g) and $CH_3C{\equiv}CCH_3$ (2 mL) by heating for 7 h at 50 °C in C_6H_6 (30 mL): yellow-brown crystals (0.42 g); mp 193–195 °C; NMR (CD_2Cl_2) δ 4.70 (C_5H_5, s), 1.92 and 1.64 (2 CCH_3, s, bd), and 6.5–7.4 (C_6H_5, complex). Anal. Calcd for $C_{41}H_{36}PCo$: C, 79.60; H, 5.87. Found: C, 80.04; H, 5.96.

4. Preparation of (Triethylphosphine)cobaltacyclopentadienes. 1c (158 mg, 0.21 mmol) and PEt_3 (150 mg) were reacted in a toluene solution (15 mL) at 100 °C. After 6 h, the orange-brown reaction mixture was concentrated and then chromatographed on alumina (deactivated with 5% of H_2O, 1.5 × 10 cm). Elution with hexane-C_6H_6 (1/2) mixture gave an orange-brown band. After evaporation of the eluted solution, crystallization from CH_2Cl_2-hexane gave red crystals of $(\overline{CoCPh{=}CPhCPh{=}C}Ph)(\eta^5\text{-}C_5H_5)(PEt_3)$ (83.5 mg, 65% yield): mp 176–178 °C; NMR ($CDCl_3$) δ 4.64 (C_5H_5, s), 1.87 (PCH_2, d of q, J_{PH} = 7.5, J_{HH} = 7.5 Hz), 1.05 ($PCCH_3$, d of t, J_{PH} = 14, J_{HH} = 7 Hz), and 6.4–7.2 (C_6H_5, complex). Anal. Calcd for $C_{39}H_{40}PCo$: C, 78.25; H, 6.73. Found: C, 78.55; H, 6.80.

The PEt_3 complexes from **1a** and **1b** were prepared similarly. $(\overline{CoCPh{=}CMeCMe{=}C}Ph)(\eta^5\text{-}C_5H_5)(PEt_3)$: mp 185–187 °C; NMR ($CDCl_3$) δ 4.48 (C_5H_5, s), 1.70 (CCH_3 and PCH_2, complex), 1.95 ($PCCH_3$, d of t, J_{PH} = 14, J_{HH} = 7 Hz), and 7.0–7.4 (C_6H_5, complex). Anal. Calcd for $C_{29}H_{36}PCo$: C, 73.40; H, 7.65. Found: C, 73.62; H, 7.71. $(\overline{CoCPh{=}CMeCPh{=}C}Ph)(\eta^5\text{-}C_5H_5)(PEt_3)$: mp 155–157 °C; NMR ($CD_2Cl_2$) δ 4.58 (C_5H_5, s), 1.80 (PCH_2, d of q, J_{PH} = 7, J_{HH} = 7 Hz), 1.63 (CCH_3, s, bd), 1.00 ($PCCH_3$, d of t, J_{PH} = 14, J_{HH} = 7 Hz), and 6.8–7.4 (C_6H_5, complex). Anal. Calcd for $C_{34}H_{38}PCo$: C, 76.11; H, 7.14. Found: C, 76.54; H, 7.22.

5. Preparation of Phosphite Cobaltacyclopentadiene Complexes. (a) **3ca.** In a benzene solution (20 mL), **1c** (0.985 g, 1.33 mmol) and **2a** (1.6 g, 13 mmol) were heated at 80 °C for 5 h. The reaction mixture turned from brown to red. The mixture was concentrated under reduced pressure and the residue was chromatographed on alumina (2.5 × 15 cm). An orange band was eluted with a benzene-CH_2Cl_2 (9/1) mixture. Concentration of the solvent (to ca. 15 mL) and addition of hexane gave red crystals of **3ca** (0.748 g, 1.24 mmol, 93% yield). The second orange band, which was eluted with benzene-ethyl acetate (1/1) mixture, gave a red-orange solid (0.045 g) after evaporation of the solvent. The solid was identified to be a mixture of **4ca-1** and **4ca-2** by NMR spectroscopy.

IR (KBr): **3ca**, 3065, 3030, 2960, 2855, 1946, 1880, 1818, 1602, 1592, 1572, 1520, 1512, 1482, 1462, 1440, 1390, 1360, 1264, 1200, 1177, 1156, 1118, 1080, 1055, 1040, 1024, 998, 908, 860, 840, 820, 812, 798, 780, 770, 740, 698, 625, 600, 555 cm^{-1}; **4ca-1**, 3070, 3040, 2960, 2850, 1602, 1498, 1448, 1422, 1410, 1386, 1350, 1311, 1280, 1198, 1188, 1178, 1158, 1112, 1078, 1070, 1045, 1010, 995, 830, 812, 790, 760, 740, 710, 692, 665, 645, 612, 602, 585, 564, 522, 500 cm^{-1}; **4ca-2**, 3080, 3000, 2960, 2850, 1600, 1580, 1498, 1450, 1412, 1386, 1350, 1310, 1212, 1190, 1174, 1165, 1110, 1098, 1070, 1010, 972, 910, 848, 830, 820, 804, 792, 770, 760, 740, 720, 702, 692, 635, 610, 588, 565, 515 cm^{-1}.

(b) **3ha.** A toluene (10 mL) solution of **1h** (103 mg, 0.15 mmol) and **2a** (0.4 g) was heated at 100 °C with stirring. After 9 h, the solution was concentrated under reduced pressure and the red residue was chromatographed on alumina (1.0 × 12 cm). A yellow-orange band eluted with a benzene-ethyl acetate (4/1) mixture was collected. After evaporation to dryness, crystallization from benzene-hexane gave yellow crystals of **3ha** (67 mg, 0.12 mmol, 80% yield). Elution with a benzene-ethyl acetate (1/1) mixture gave a small amount of a red-orange solution. The eluate, after evaporation and crystallization from benzene-hexane, gave **4ha** (2 mg). **3ia**, **3fa**, and **3ga** were prepared similarly.

6. Preparation of 1-Alkoxyphosphole Oxide Complexes. (a) **4ca.** A xylene (15 mL) solution of **3ca** (462 mg, 0.76 mmol) was stirred at 120 °C. After 6.5 h, the solvent was removed under reduced pressure and the residue was chromatographed on alumina (1.5 × 15 cm). Elution with hexane-benzene (3/1 to 1/1) mixture gave a yellow and an orange band. The yellow eluate, after evaporation to dryness and crystallization of the residue from benzene-hexane, gave yellow crystals of (η^5-cyclopentadienyl)(η^4-tetraphenylcyclobutadiene)cobalt (**5**, 81 mg, 0.17 mmol). From the orange eluate, the unreacted **3ca** (181 mg, 0.30 mmol) was recovered by similar workup. Elution with a benzene-ethyl acetate (7/3) mixture gave two orange bands. From the more readily eluted orange band, after evaporation of the solvent and crystallization from benzene-hexane, orange crystals of **4ca-1** (38 mg, 0.07 mmol) were obtained. The second band was eluted with a benzene-ethyl acetate (1/1) mixture. Evaporation of the solvent and crystallization gave **4ca-2** (102 mg, 0.18 mmol).

A similar treatment of **3ca** (410 mg, 0.68 mmol) in the presence of **2a** (1 mL) gave unreacted **3ca** (196 mg) and **4ca-1** (25 mg) and **4ca-2** (110 mg).

(b) **4da.** In a benzene (30 mL) solution, **1d** (420 mg, 0.85 mmol) and **2a** (650 mg, 5.2 mmol) were heated at 80 °C for 6 h. The color of the solution changed from brown to light orange. After evaporation of the solvent, the orange residue was chromatographed on alumina (deactivated with 5% of H_2O, 1.5 × 15 cm). After a small amount of pale orange band eluted with benzene, a yellow band was eluted with a benzene-THF (1/1) mixture. Evaporation of the solvent, followed by crystallization from benzene-hexane, gave yellow crystals of **4da-2** (180 mg, 0.58 mmol, 68% yield).

(c) **4cg.** In a toluene (20 mL) solution, **1c** (833 mg, 1.12 mmol) and **2g** (1.8 g, 5.8 mmol) were stirred at 90 °C for 6 h. The solution changed from dark brown to orange. After concentration of the solvent, the residue was chromatographed on alumina (2.5 × 20 cm). After a trace amount of pale yellow band eluted with a hexane-benzene (1/1) mixture, two orange bands were separated with a benzene-ethyl acetate (3/2) mixture. The first band was eluted with the same mixture and evaporated to dryness. Crystallization of the residue from benzene-hexane gave orange crystals of **4cg-1** (90 mg, 0.15

mmol). The second orange band was eluted with a benzene-ethyl acetate (1/4) mixture. A similar workup gave orange crystals of **4cg-2** (533 mg, 0.86 mmol).

(**d**) **4ha.** In a toluene (15 mL) solution, **1h** (320 mg, 0.45 mmol) and **2a** (1 mL) were reacted at 120 °C for 7 h. After evaporation of the solvent, the red residue was chromatographed on alumina (1.5 × 12 cm). From a yellow-orange band which was eluted with a benzene-ethyl acetate (5/1) mixture, **3ha** (143 mg, 0.25 mmol) was isolated. From a red-orange band eluted with a benzene-ethyl acetate (1/1) mixture **4ha** (31 g, 0.06 mmol) was obtained.

(**e**) **Reaction Products of 1c with 2e or 2f.** In a benzene (30 mL) solution, **1c** (457 mg, 0.62 mmol) was reacted with **2e** (0.8 g, 6.6 mmol) at 85 °C. After 10 h, the reaction mixture was evaporated to dryness. The red residue was dissolved in CH_2Cl_2 (3 mL) and chromatographed on alumina (deactivated with 10% of H_2O, 1.5 × 15 cm). Elution with benzene-THF (6/1 and 1/1) mixtures gave two orange bands from which **4ca-1** (18 mg, 0.03 mmol) and **4ca-2** (56 mg, 0.10 mmol) were isolated. A broad, orange band eluted with THF was collected and the eluate, after concentration, was rechromatographed on silica gel. The first orange band eluted with ethyl acetate gave orange crystals. **4ce-1** (71 mg, 0.12 mmol) and the second orange band eluted with an ethyl acetate-THF (2/1) mixture gave orange crystals, **4ce-2** (56 mg, 0.10 mmol). Analysis and IR and NMR spectra of the products showed **4ce-1** and **4ce-2** to be the endo and exo isomers of the 1-(2-hydroxyethyloxy)-2,3,4,5-tetraphenylphosphole oxide complex of η^5-C_5H_5Co. **4ce-1:** mp 258-260 °C; $\nu_{P=O}$ 1172, ν_{OH} 3260 cm^{-1}; NMR ($CDCl_3$) δ 4.91 (C_5H_5, s), 4.29 ($POCH_2$, d of t, J_{PH} = 10.8, J_{HH} = 6 Hz) 3.75 (-CH_2OH, t), ~3.75 (OH), 6.9-7.4 (C_6H_5, complex). Anal. Calcd for $C_{35}H_{30}O_3PCo$: C, 71.43; H, 5.13. Found: C, 71.34; H, 5.20. **4ce-2:** mp 239-241 °C; $\nu_{P=O}$ 1198, ν_{OH} 3260 cm^{-1}; NMR ($CDCl_3$) δ 4.90 (C_5H_5, s), 3.80 ($POCH_2$, d of m, J_{PH} = 10 Hz), 3.52 (-CH_2OH, m) 6.9-7.4 (C_6H_5, complex). Anal. Found: C, 71.20; H, 5.17.

The reaction of **1c** (413 mg, 0.56 mmol) and **2f** (0.85 g, 6.3 mmol) gave the *exo*-1-(3-hydroxypropyloxy) analogue **4cf-2** (124 mg, 0.21 mmol) besides **4ca-1** (20 mg, 0.04 mmol) and **4ca-2** (56 mg, 0.10 mmol). **4cf-2:** mp 197-201 °C; $\nu_{P=O}$ 1200, ν_{OH} 3300 cm^{-1}; NMR ($CDCl_3$) δ 4.88 (C_5H_5, s), 3.90 ($POCH_2$, d of t, J_{PH} = 9.0, J_{HH} = 6.0 Hz), 3.34 (-CH_2OH, t, J_{HH} = 6.0 Hz), ~3.35 (OH), 1.57 (CCH_2C, t of t, J_{HH} = 6.0 Hz), 6.9-7.4 (C_6H_5, complex). Anal. Calcd for $C_{36}H_{32}O_3PCo$: C, 71.74; H, 5.36. Found: C, 71.52; H, 5.39.

7. **Thermolysis of Crystals (a). 4cd.** Crystals of **3cd** (192 mg, 0.31 mmol) were heated in an ampule at 210 °C for 1 h, yielding a red mass. The solid was dissolved in CH_2Cl_2 (3 mL) and chromatographed on silica gel (1.0 × 15 cm). From a pale yellow band eluted with a hexane-benzene (2/1) mixture, after evaporation and crystallization from benzene-hexane, yellow crystals of **5** (1 mg) were obtained. An orange broad band was eluted with benzene-THF mixtures (8/1 to 6/1). Evaporation of the solvent gave a noncrystalline red residue (175 mg) whose NMR spectrum showed the presence of signals assignable to two kinds of complexes with unidentified contaminants. The residue was rechromatographed on silica gel (1.0 × 20 cm). After thorough elution with benzene, the first orange band eluted with benzene-THF (20/1) mixture gave red-orange crystals of **4cd-1** (23 mg, 0.04 mmol) by crystallization from benzene-hexane. The second orange band eluted with a benzene-THF (7/1) mixture gave orange crystals of **4cd-2** (86 mg, 0.14 mmol).

(**b**) **4cb.** A similar treatment of **3cb** (200 mg, 0.31 mmol) at 180-190 °C for 1 h followed by chromatography on alumina gave a yellow band and two orange bands by elution with hexane-benzene (1/1) and benzene-ethyl acetate (3/2 and 2/3) mixtures. From these eluates, **5** (59 mg, 39% yield), **4cb-1** (19 mg, 0.03 mmol, 10% yield), and **4cb-2** (84 mg, 0.15 mmol, 48% yield) were isolated, respectively. When **3cb** was heated at higher temperature (210-220 °C), the amount of **5** increased (to 67% yield) and that of **4cb-2** decreased (to 28% yield). A similar treatment in the presence of an excess of **2b** gave **4cb-1** (6% yield) and **4cb-2** (90% yield) and no formation of **5**.

8. **Photochemical Preparations. (a) 3ba.** A solution of **1b** (318 mg, 0.47 mmol) and **2a** (0.5 mL) in CH_2Cl_2 (30 mL) was irradiated (Rikō Kagaku 100-W high-pressure mercury lamp, cutoff filter L-39, Toshiba, λ >350 nm) while being stirred at room temperature in a Pyrex tube, which was placed 10 cm from the lamp. After irradiation for 4 days, the reaction mixture was concentrated (to 5 mL) and chromatographed on alumina (deactivated wth 10% of H_2O, 1.5 × 10 cm). Elution with a hexane-CH_2Cl_2 (3/1) mixture gave an orange band. Evaporation of the solvent under reduced pressure at room temperature and crystallization from benzene-hexane gave orange crystals of **3ba** (217 mg, 0.40 mmol).

Table VI. Molecular Geometry for **4ca-2**

A. Intramolecular Distances (Å), with Estimated Standard Deviations in Parentheses

Co-C(2)	2.073(6)	O(1)-C(1)	1.441(7)
Co-C(3)	2.004(4)	C(2)-C(3)	1.445(7)
Co-C(4)	1.990(4)	C(3)-C(4)	1.440(7)
Co-C(5)	2.047(4)	C(4)-C(5)	1.436(5)
Co-C(11)	2.082(7)	C(11)-C(12)	1.400(10)
Co-C(12)	2.053(6)	C(12)-C(13)	1.400(8)
Co-C(13)	2.048(5)	C(13)-C(14)	1.419(9)
Co-C(14)	2.064(4)	C(14)-C(15)	1.451(10)
Co-C(15)	2.059(6)	C(15)-C(11)	1.411(7)
P-O(1)	1.607(3)	C(2)-C(21)	1.476(8)
P-O(2)	1.484(3)	C(3)-C(31)	1.501(5)
P-C(2)	1.764(4)	C(4)-C(41)	1.485(7)
P-C(5)	1.772(6)	C(5)-C(51)	1.496(7)

B. Intramolecular Angles (deg), with Estimated Standard Deviations in Parentheses

C(2)-Co-C(5)	74.6(2)	C(2)-C(3)-C(4)	112.2(4)
C(3)-Co-C(4)	42.3(2)	C(3)-C(4)-C(5)	110.9(4)
O(1)-P-O(2)	110.5(2)	C(21)-C(2)-C(3)	125.1(4)
O(1)-P-C(2)	105.8(2)	C(2)-C(3)-C(31)	125.6(4)
O(1)-P-C(5)	109.8(2)	C(3)-C(4)-C(41)	122.3(4)
O(2)-P-C(2)	120.4(2)	C(41)-C(4)-C(5)	126.5(4)
O(2)-P-C(5)	118.5(2)	C(4)-C(5)-C(51)	126.4(4)
P-O(1)-C(1)	119.4(3)	C(11)-C(12)-C(13)	108.4(5)
P-C(2)-C(3)	107.5(3)	C(12)-C(13)-C(14)	109.3(5)
P-C(5)-C(4)	108.5(3)	C(13)-C(14)-C(15)	106.1(5)
P-C(2)-C(21)	125.2(4)	C(15)-C(11)-C(12)	108.6(5)
P-C(5)-C(51)	121.2(3)		

C. Equations of Least-Squares Planes, Which Are in Cartesian Coordinates (Å) with the z Axis Coinciding with c and the y Axis Coinciding with b^*[a]

plane (1): C(2)-C(5)

$0.1660X + 0.0541Y + 0.9846Z - 1.51566 = 0$

[Co −1.594, P 0.632, C(2) −0.003, C(3) 0.005, C(4) −0.005, C(5) 0.003]

plane (2): C(11)-C(15)

$0.2782X - 0.0118Y + 0.9604Z + 1.44321 = 0$

[C(11) −0.014, C(12) 0.011, C(13) −0.004, C(14) −0.004, C(15) 0.011]

plane (3): P, C(2), C(5)

$0.5748X - 0.2084Y + 0.7913Z - 2.25656 = 0$

angles (deg) between planes:

(1)-(2) 7.6 (1)-(3) 30.3

[a] Distances (Å) of relevant atoms from the plane are shown in square brackets.

(**b**) **4da.** A solution of **1d** (108 mg, 0.22 mmol) and **2a** (180 mg, 1.5 mmol) in benzene (15 mL) was similarly irradiated. The color of the solution changed from dark brown to light orange. The reaction mixture was concentrated at room temperature and chromatographed on alumina (deactivated with 10% of H_2O, 1.3 × 10 cm). After the column was eluted thoroughly with hexane-CH_2Cl_2 mixtures, a yellow band was eluted with a CH_2Cl_2-THF (1/1) mixture. Evaporation of the solvent followed by crystallization from benzene-hexane gave yellow crystals of **4da-2** (56 mg, 0.18 mmol).

9. **Cleavage.** A solution of **4cd-2** (125 mg, 0.2 mmol) in CH_2Cl_2-$(CH_3)_2CO$ (1/1) mixture (20 mL) was stirred with $Ce(NO_3)_4 \cdot 2(NH_4NO_3) \cdot xH_2O$ (0.5 g) at room temperature for 1 day. The orange solution changed to pale orange. The mixture was evaporated to dryness and the residue was extracted with CH_2Cl_2 (10 mL). The yellow extract, after concentration (to ~3 mL), was chromatographed on alumina. Elution with C_6H_6-THF (4/1) mixture gave a yellow band. Concentration of the eluate to about 3 mL, followed by addition of hexane (10 mL), gave yellow crystals of 1-[3-(3-methyl)oxetanyl]methyloxy-2,3,4,5-tetraphenylphosphole oxide (7.26 mg, 0.14 mmol, 73% yield).

A solution of **4cb-2** (270 mg, 0.45 mmol) in toluene (10 mL) was

Table VII. Final Atomic Parameters and Their Standard Deviations[a]

atom	x	y	z	B_{11}	B_{22}	B_{33}	B_{12}	B_{13}	B_{23}
Co	0.342 50(8)	0.296 67(5)	0.057 39(8)	2.35(3)	2.64(3)	2.62(3)	−0.51(2)	1.03(2)	0.20(2)
P	0.222 90(12)	0.357 64(8)	0.249 35(12)	1.81(5)	2.33(4)	2.86(5)	−0.37(4)	0.95(4)	0.02(4)
O1	0.2588(3)	0.3539(2)	0.4170(3)	3.41(1)	3.7(1)	2.6(1)	−0.9(1)	1.5(1)	−0.4(1)
O2	0.0688(2)	0.4109(2)	0.1720(3)	1.1(1)	3.4(1)	4.5(1)	−0.1(1)	0.5(1)	0.8(1)
C1	0.1970(6)	0.4412(4)	0.4813(6)	4.5(3)	5.7(3)	5.3(3)	−1.8(2)	2.7(2)	−2.3(2)
C2	0.3040(4)	0.2357(3)	0.2098(4)	2.3(2)	2.5(1)	2.7(2)	−0.8(1)	1.1(1)	0.1(1)
C3	0.4532(4)	0.2207(3)	0.2452(4)	2.3(2)	2.6(2)	2.9(2)	−0.2(1)	1.0(1)	0.3(1)
C4	0.4789(4)	0.3125(3)	0.2461(4)	2.0(2)	2.6(2)	3.0(2)	−0.4(1)	1.1(1)	0.3(1)
C5	0.3485(4)	0.3952(3)	0.2137(4)	1.9(1)	2.5(1)	2.9(2)	−0.7(1)	1.1(1)	0.1(1)
C11	0.4198(5)	0.2747(4)	−0.1061(5)	4.8(3)	5.0(3)	3.8(2)	−0.8(2)	2.7(2)	0.0(2)
C12	0.3475(5)	0.2092(3)	−0.1108(5)	4.9(3)	3.6(2)	4.0(2)	−0.9(2)	2.1(2)	−0.5(2)
C13	0.2063(6)	0.2648(4)	−0.1284(5)	5.0(3)	6.3(3)	3.1(2)	−2.7(2)	1.1(2)	−0.6(2)
C14	0.1881(5)	0.3670(4)	−0.1315(5)	4.4(2)	5.6(3)	2.1(2)	−0.1(2)	0.3(2)	0.4(2)
C15	0.3256(6)	0.3724(4)	−0.1151(5)	5.5(3)	4.9(2)	3.2(2)	−1.8(2)	1.8(2)	0.7(2)
C21	0.2420(4)	0.1561(3)	0.1865(4)	2.4(2)	2.7(2)	2.3(2)	−0.8(1)	0.6(1)	0.4(1)
C22	0.1186(5)	0.1733(3)	0.2148(5)	2.8(2)	3.3(2)	4.0(2)	−0.9(1)	1.3(2)	0.3(1)
C23	0.0576(5)	0.1007(3)	0.2019(5)	3.1(2)	4.2(2)	5.8(3)	−1.8(2)	1.5(2)	0.1(2)
C24	0.1173(5)	0.0100(4)	0.1550(5)	4.8(3)	4.3(2)	5.2(3)	−2.7(2)	1.2(2)	0.1(2)
C25	0.2388(6)	−0.0081(3)	0.1234(6)	5.5(3)	3.4(2)	5.7(3)	−2.0(2)	2.3(2)	−0.8(2)
C26	0.2976(5)	0.0649(3)	0.1355(5)	4.1(2)	2.9(2)	4.8(2)	−1.5(2)	2.3(2)	−0.9(2)
C31	0.5725(4)	0.1231(3)	0.2873(4)	2.4(2)	2.4(2)	3.6(2)	−0.2(1)	1.3(1)	0.2(1)
C32	0.6708(5)	0.0889(3)	0.2227(5)	3.2(2)	3.2(3)	−0.0(1)	−0.0(1)	2.3(2)	0.3(2)
C33	0.7852(5)	−0.0002(3)	0.2754(6)	3.4(2)	3.7(2)	8.0(4)	0.4(2)	3.1(2)	−0.2(2)
C34	0.7952(6)	−0.0530(4)	0.3886(7)	4.0(3)	3.7(2)	8.8(4)	1.0(2)	1.6(3)	1.7(2)
C35	0.6978(6)	−0.0186(4)	0.4550(6)	4.4(3)	4.7(3)	7.1(3)	0.2(2)	1.3(2)	2.7(2)
C36	0.5823(5)	0.0697(3)	0.4029(5)	3.4(2)	4.3(2)	4.2(2)	0.1(2)	1.3(2)	1.7(2)
C41	0.6251(4)	0.3171(3)	0.2919(4)	2.3(2)	2.5(2)	3.4(2)	−0.5(1)	1.2(1)	−0.2(1)
C42	0.6728(5)	0.3545(3)	0.2059(5)	2.5(2)	3.5(2)	4.5(2)	−0.8(1)	1.5(2)	0.3(2)
C43	0.8100(5)	0.3586(3)	0.2593(5)	3.3(2)	3.7(2)	6.1(3)	−1.3(2)	2.6(2)	−0.4(2)
C44	0.8980(5)	0.3268(3)	0.3955(6)	2.7(2)	4.3(2)	6.3(3)	−1.5(2)	1.8(2)	−1.3(2)
C45	0.8518(5)	0.2899(4)	0.4825(5)	2.5(2)	4.5(2)	5.4(3)	−0.6(2)	0.7(2)	−0.7(2)
C46	0.7162(4)	0.2844(3)	0.4308(5)	2.3(2)	3.6(2)	3.6(2)	−0.7(1)	0.9(1)	−0.1(1)
C51	0.3332(4)	0.5021(3)	0.2073(4)	2.6(2)	2.5(2)	2.8(2)	−0.7(1)	1.3(1)	−0.0(1)
C52	0.2056(5)	0.5684(3)	0.1124(5)	2.7(2)	2.9(2)	3.8(2)	−0.6(1)	0.5(1)	0.5(1)
C53	0.1866(5)	0.6693(3)	0.1125(5)	3.8(2)	3.0(2)	4.8(2)	−0.4(2)	1.2(2)	0.9(2)
C54	0.2876(5)	0.7044(3)	0.2029(5)	4.9(3)	2.5(2)	5.6(3)	−0.7(2)	2.9(2)	−0.1(2)
C55	0.4142(5)	0.6396(3)	0.2983(5)	3.5(2)	3.7(2)	5.4(3)	−1.6(2)	2.2(2)	−0.9(2)
C56	0.4357(4)	0.5387(3)	0.3008(5)	2.5(2)	3.1(2)	3.8(2)	−1.1(1)	1.1(1)	−0.6(1)
H1A	0.090(5)	0.472(3)	0.425(5)	7.1(14)					
H1B	0.256(6)	0.490(4)	0.498(6)	10.6(18)					
H1C	0.211(5)	0.411(3)	0.558(5)	7.5(14)					
H11	0.535(5)	0.263(3)	−0.080(5)	7.8(15)					
H12	0.394(4)	0.144(3)	−0.101(4)	4.7(12)					
H13	0.137(5)	0.237(3)	−0.120(5)	6.3(13)					
H14	0.083(6)	0.429(4)	−0.129(6)	9.7(18)					
H15	0.368(5)	0.435(3)	−0.094(5)	8.1(15)					
H22	0.083(4)	0.234(3)	0.268(4)	5.4(12)					
H23	−0.033(4)	0.118(3)	0.234(4)	5.6(12)					
H24	0.078(6)	−0.049(4)	0.136(6)	8.9(18)					
H25	0.276(5)	−0.076(3)	0.073(5)	6.7(14)					
H26	0.383(5)	0.049(3)	0.103(5)	6.7(14)					
H32	0.664(5)	0.130(3)	0.136(4)	6.0(13)					
H33	0.861(5)	−0.024(3)	0.223(4)	5.8(13)					
H34	0.881(6)	−0.121(4)	0.428(6)	10.1(18)					
H35	0.680(6)	−0.064(4)	0.522(6)	11.0(20)					
H36	0.524(4)	0.094(3)	0.476(4)	4.3(11)					
H42	0.612(4)	0.374(3)	0.107(4)	4.3(11)					
H43	0.830(5)	0.379(3)	0.188(5)	6.5(14)					
H44	0.997(4)	0.335(3)	0.439(4)	4.8(11)					
H45	0.915(8)	0.273(5)	0.572(8)	16.0(29)					
H46	0.671(5)	0.262(3)	0.496(5)	6.4(13)					
H52	0.124(4)	0.546(3)	0.050(4)	4.1(11)					
H53	0.093(4)	0.713(3)	0.053(4)	5.8(13)					
H54	0.280(5)	0.771(3)	0.220(5)	6.3(13)					
H55	0.486(5)	0.669(3)	0.373(5)	6.2(13)					
H56	0.536(4)	0.494(3)	0.371(4)	5.2(12)					

[a] The temperature factors for heavier atoms are of the form $T = \exp[-\frac{1}{4}(B_{11}h^2a^{*2} + B_{22}k^2b^{*2} + B_{33}l^2c^{*2} + 2B_{12}hka^*b^* + 2B_{13}hla^*c^* + 2B_{23}klb^*c^*)]$, and those for the hydrogen atoms are $T = \exp[-B(\sin\theta/\lambda)^2]$.

heated with I_2 (0.37 g, 1.46 mmol) at 80°C for 15 h. A similar workup gave 1-ethoxy-2,3,4,5-tetraphenylphosphole oxide (23 mg, 0.05 mmol, 35% yield) together with the unreacted **4cb-2** (184 mg), showing that I_2 is less effective for the cleavage. Me_3NO was found to be inactive.

10. Isomerization. Crystals of **4cb-1** (50 mg) were placed in a capped flask and heated to 280–290 °C for 10 min, giving a dark red oil. After cooling, the red solid was dissolved in a small amount of CH_2Cl_2 and chromatographed on alumina. Elution with C_6H_6 followed by C_6H_6–ethyl acetate mixture gave the unchanged **4cb-1** (24 mg) and the isomerization product **4cb-2** (8 mg, in a 16% conversion). The red oil obtained from **4cb-2** by similar treatment showed only the signals of **4cb-2** in the NMR spectrum and no signals attributable to the formation of any other C_5H_5 protons. Isomerizations of **4ca-1** and **4cg-1** were similarly checked. No isomerization of **4ch-1** was observed up to 310 °C.

11. Kinetic Procedures. The kinetics of the substitution reactions and of the conversion reactions were studied in CD_2Cl_2 solution using an NMR method for analysis. The extent of reaction was estimated from the signal heights of the C_5H_5 protons of the unreacted complex and of the product complex or complexes. For the substitution reaction runs, the starting triphenylphosphine complex was dissolved in CD_2Cl_2 (0.3 mL) by heating for a short time in an NMR tube fitted with a tightly fitting stopper and then adding the phosphite. After further addition of CD_2Cl_2 containing tetramethylsilane to fix the total volume to 0.5 mL, the tube was sealed. For the conversion reaction runs, the phosphite complex and phosphite were placed in a tube and dissolved in CD_2Cl_2 containing tetramethylsilane (total volume 0.5 mL) and the tube was sealed. The rate measurements were carried out at the concentration range 0.10–0.15 M of the starting complexes. The sealed tube was placed in the constant-temperature bath with a regulation of ±0.02 °C using Shin Etsu Silicon KF-98 of 50 cS as a medium. The spectrum was recorded at suitable intervals on a Varian HA-100B spectrometer; the signal heights of the C_5H_5 protons were recorded seven times and the five intermediate ones were averaged. The rate constant was computed by the method of least squares.

12. X-ray Study of 4ca-2. Crystals suitable for an X-ray analysis were grown from a C_6H_6–hexane solution. The crystal used was columnar with dimensions 0.37 × 0.09 × 0.13 mm along the a^*, b^*, and c^*, respectively. Preliminary Weissenberg photographs showed that the crystal was triclinic of space group $P1$ or $P\bar{1}$. The space group $P\bar{1}$ was confirmed by a successful refinement.

The unit cell constants of a = 10.737 (6) Å, b = 14.413 (5) Å, c = 10.194 (3) Å, α = 94.48 (3)°, β = 111.87 (3)°, γ = 69.98 (4)° were determined from high-order reflections on a Rigaku four-circle automatic diffractometer. The unit cell volume is 1373.2 Å^3, yielding a calculated density of 1.351 g cm^{-3} for $CoPO_2C_{34}H_{28}$ (mol wt 558.508) and Z = 2. The experimental density as determined by flotation in an aqueous solution of KI was found to be 1.33 g cm^{-3}. The crystal was mounted such that the a axis was nearly parallel to the ϕ axis of the diffractometer. The intensity data were collected by the $2\theta/\omega$ scan method using Cu Kα radiation monochromated by graphite crystal. A scan rate of 4° min^{-1} was used. Ten-second stationary background counts were taken at the lower and upper limits of each scan. Three standard reflections were monitored before every 100 measurements. A total of 4129 independent intensities in the range 6° ≤ 2θ < 140° were measured. The treatment of the intensity data has been previously described.[26] The 3719 reflections for which $F_o > 3\sigma(F_o)$ were used in the solution and refinement of the structure. Intensities were corrected for Lorentz and polarization effects. The linear absorption coefficient of the compound for Cu Kα was 62.06 cm^{-1}, and absorption correction was made. The calculated transmission factors varied from 0.776 to 0.887.

The coordinates of the cobalt and phosphorus atoms were determined from a sharpened Patterson map.[27] The subsequent structure factor and electron density map calculations revealed the positions of other atoms except hydrogens. Five cycles of a block-diagonal least-squares refinement of all the positional and isotropic thermal parameters resulted in the residual factors $R_1 = \Sigma||F_o| - |F_c||/\Sigma|F_o|$ and $R_2 = [\Sigma w(|F_o| - |F_c|)^2/\Sigma w F_o^2]^{1/2}$ of 10.7 and 11.7% using unit (equal) weight, respectively. Subsequent five cycles of a refinement involving anisotropic thermal parameters converged to R_1 = 8.38 and R_2 = 8.25%. At this stage a difference-Fourier synthesis revealed all of the 28 hydrogen atoms in the molecule. Six more cycles of a block-diagonal least-squares calculations completed the refinement, in which the 28 hydrogen atoms with isotropic thermal parameters were included. This refinement converged to the lower residual factors R_1 = 6.36 and R_2 = 5.39%. In these refinements, the $\Sigma w(|F_o| - |F_c|)^2$ function was minimized, where the weight, w, was $1/\sigma(F_o)$. No unusual trends were observed in an analysis of $\Sigma w(|F_o| - |F_c|)^2$ as a function of either θ/λ or $|F_o|$. In the final cycles of a refinement, no positional parameter exhibited shifts of more than 0.50 and 0.58 times its standard deviation for nonhydrogen atoms and for hydrogen atoms, respectively. The standard deviation of an observation of unit weight, $[\Sigma w(|F_o| - |F_c|)^2/(m - n)]^{1/2}$, was 1.92, where the number of reflections (m) and refined parameters (n) were 3719 and 455, respectively. Anomalous dispersion effects for Co and P were included in the calculation of F_c using $\Delta f'$ and $\Delta f''$ calculated by Cromer.[28] The atomic scattering factors used were from the usual tabulation.[29]

A list of observed and calculated structure factor amplitudes is available.[30] The final atomic coordinates and thermal parameters are listed in Table VI, and the selected bond distances and bond angles are shown in Table VII.

Supplementary Material Available: A listing of the observed and calculated structure amplitudes for **4ca-2** (12 pages). Ordering information is given on any current masthead page.

References and Notes

(1) For the preceding paper in this series, see: Yamazaki, H.; Wakatsuki, Y. *Bull. Chem. Soc. Jpn.* **1979**, *52*, 1239.
(2) Vollhart, K. P. C. *Acc. Chem. Res.* **1977**, *10*, 1, and references cited therein.
(3) Wakatsuki, Y.; Yamazaki, H. *Tetrahedron Lett.* **1973**, 3383.
(4) Bönnemann, H. *Angew. Chem., Int. Ed. Engl.* **1978**, *17*, 505.
(5) Yamazaki, H.; Wakatsuki, Y. *J. Organomet. Chem.* **1977**, *139*, 157.
(6) McDonnell Bushnell, L. P.; Evitt, E. R.; Bergman, R. G. *J. Organomet. Chem.* **1978**, 157, 445.
(7) Wakatsuki, Y.; Yamazaki, H. *J. Organomet. Chem.* **1977**, *139*, 169.
(8) Wakatsuki, Y.; Yamazaki, H. *J. Chem. Soc., Chem. Commun.* **1978**, 280.
(9) Wakatsuki, Y.; Yamazaki, H. *J. Chem. Soc., Dalton Trans.* **1978**, 1278.
(10) Hong, P.; Yamazaki, H. *Nippon Kagaku Kaishi* **1978**, 730.
(11) McAlister, D. R.; Bercow, J. E.; Bergman, R. G. *J. Am. Chem. Soc.* **1977**, *99*, 1666.
(12) The suffix **aa** in **3aa** means that the complex is derived from **1a** and **2a**. The same rule is applied to **4**.
(13) Barrow, M. J.; Freer, A. A.; Harrison, W.; Sim, G. A.; Taylor, D. W.; Wilson, F. B. *J. Chem. Soc., Dalton Trans.* **1975**, 196.
(14) The formation of pentaphenylphosphole oxide by reacting $Fe_2(CO)_6$-$(PhC_2Ph)_2$ with $PhPCl_2$ has been reported: Braye, E. H.; Hübel, W. *Chem. Ind. (London)* **1959**, 1250.
(15) Leavitt, F. C.; Manuel, T. A.; Johnson, F.; Matternas, L. U.; Lehman, D. S. *J. Am. Chem. Soc.* **1960**, *82*, 5099.
(16) Braye, E. H.; Hübel, W.; Caplier, I. *J. Am. Chem. Soc.* **1961**, *83*, 4406.
(17) The cyclic phosphites **2e** and **2f** also were found to show the same order of reactivity in the reaction 1, although they are not plotted in Figure 2 since overlapping of the signals of the Cp protons and the protons of CH_2 moieties of the products prevented accurate estimation of their rates.
(18) Tolman, C. A. *Chem. Rev.* **1977**, *77*, 313.
(19) Barrow, M. J.; Davidson, J. L.; Harrison, W.; Sharp, D. W. A.; Sim, G. A.; Wilson, F. B. *J. Chem. Soc., Chem. Commun.* **1973**, 583.
(20) Emsley, J.; Hall, C. "The Chemistry of Phosphorus"; Harper and Row: New York, 1976; (a) Chapter 4; (b) Chapter 5, p 219.
(21) Denney, D. B.; Jones, D. H. *J. Am. Chem. Soc.* **1969**, *91*, 5821.
(22) Denney, D. B.; Denney, D. A.; Hall, C. D.; Marsi, K. L. *J. Am. Chem. Soc.* **1972**, *94*, 245.
(23) Denney, D. Z.; Chen, G. Y.; Denney, D. B. *J. Am. Chem. Soc.* **1969**, *91*, 6838.
(24) Coyne, D. M.; McEwen, W. E.; vander Werf, G. A. *Justus Liebigs Ann. Chem.* **1956**, *78*, 3061.
(25) Wakatsuki, Y.; Kuramitsu, T.; Yamazaki, H. *Tetrahedron Lett.* **1974**, 4549.
(26) Yasufuku, K.; Aoki, K.; Yamazaki, H. *Inorg. Chem.* **1977**, *16*, 624.
(27) The following programs were used during the course of structural analysis: READ 80, data reduction on a FACOM 230-75 computer, Kobayashi, K.; Sakurai, T.; ABS 10, absorption correction, Ito, T.; FANDER, structure factor calculation and Fourier syntheses, Iitaka, Y.; HBLS, structure-factor calculation and block-diagonal least-squares refinement, Ashida, T.; BOND, distances, angles, and least-squares planes, Iitaka, Y.; ORTEP, thermal ellipsoid drawings, Johnson, C. K.
(28) Cromer, D. T.; Liberman, D. *J. Chem. Phys.* **1971**, *53*, 189.
(29) "International Tables for X-ray Crystallography", Vol. 3; Kynoch Press: Birmingham, England, 1962.
(30) See paragraph at end of paper regarding supplementary material.